

## Accepted Manuscript

### Optimization of Microtubule Affinity Regulating Kinase (MARK) Inhibitors with Improved Physical Properties

David L. Sloman, Njamkou Noucti, Michael D. Altman, Dapeng Chen, Andrea C. Mislak, Alexander Szewczak, Mansuo Hayashi, Lee Warren, Tammy Dellovade, Zhenhua Wu, Jacob Marcus, Deborah Walker, Hua-Poo Su, Suzanne C. Edavettal, Sanjeev Munshi, Michael Hutton, Hugh Nuthall, Matthew G. Stanton

PII: S0960-894X(16)30106-8  
DOI: <http://dx.doi.org/10.1016/j.bmcl.2016.02.003>  
Reference: BMCL 23554

To appear in: *Bioorganic & Medicinal Chemistry Letters*

Received Date: 18 December 2015  
Accepted Date: 2 February 2016

Please cite this article as: Sloman, D.L., Noucti, N., Altman, M.D., Chen, D., Mislak, A.C., Szewczak, A., Hayashi, M., Warren, L., Dellovade, T., Wu, Z., Marcus, J., Walker, D., Su, H-P., Edavettal, S.C., Munshi, S., Hutton, M., Nuthall, H., Stanton, M.G., Optimization of Microtubule Affinity Regulating Kinase (MARK) Inhibitors with Improved Physical Properties, *Bioorganic & Medicinal Chemistry Letters* (2016), doi: <http://dx.doi.org/10.1016/j.bmcl.2016.02.003>

This is a PDF file of an unedited manuscript that has been accepted for publication. As a service to our customers we are providing this early version of the manuscript. The manuscript will undergo copyediting, typesetting, and review of the resulting proof before it is published in its final form. Please note that during the production process errors may be discovered which could affect the content, and all legal disclaimers that apply to the journal pertain.



## Optimization of Microtubule Affinity Regulating Kinase (MARK) Inhibitors with Improved Physical Properties

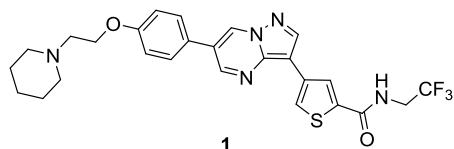
David L. Sloman\*<sup>†</sup>, Njamkou Noucti<sup>†</sup>, Michael D. Altman<sup>‡</sup>, Dapeng Chen<sup>§</sup>, Andrea C. Mislak<sup>§</sup>, Alexander Szewczak<sup>¶</sup>, Mansuo Hayashi<sup>¶</sup>, Lee Warren<sup>¶</sup>, Tammy Dellovade<sup>‡</sup>, Zhenhua Wu<sup>‡</sup>, Jacob Marcus<sup>Δ</sup>, Deborah Walker<sup>Π</sup>, Hua-Poo Su<sup>◊</sup>, Suzanne C. Edavettal<sup>◊</sup>, Sanjeev Munshi<sup>◊</sup>, Michael Hutton<sup>Δ</sup>, Hugh Nuthall<sup>Δ</sup>, Matthew G. Stanton<sup>†</sup>

Discovery Chemistry<sup>†</sup>, Chemistry Modeling and Informatics<sup>‡</sup>, Drug Metabolism and Pharmacokinetics<sup>§</sup>, Neuroscience Drug Discovery<sup>Δ</sup>, CNS Pharmacology<sup>¶</sup>, Core Pharmacology<sup>‡</sup>, Pharmaceutical Research and Development<sup>Π</sup>, Structure Determination<sup>◊</sup> Merck and Co., Inc., 33 Avenue Louis Pasteur, Boston, MA 02215, Structural Biology, 770 Sunnyside Pike, West Point, PA, 19486.

**KEYWORDS** ("MARK, Kinase, Alzheimer's disease, amine basicity, fluorine").

**ABSTRACT:** Inhibition of microtubule affinity regulating kinase (MARK) represents a potentially attractive means of arresting neurofibrillary tangle pathology in Alzheimer's disease. This manuscript outlines efforts to optimize a pyrazolopyrimidine series of MARK inhibitors by focusing on improvements in potency, physical properties and attributes amenable to CNS penetration. A unique cyclohexyldiamine scaffold was identified that led to remarkable improvements in potency, opening up opportunities to reduce MW, Pgp efflux and improve pharmacokinetic properties while also conferring improved solubility.

Alzheimer's disease remains one of the highest areas of unmet medical need.<sup>1</sup> Despite significant efforts, disease modifying therapies for AD remain elusive.<sup>2</sup> Neurofibrillary tangles (NFTs) are one of the pathological hallmarks of AD and the degree of tangle formation correlates well with cognitive decline. NFTs are composed of hyperphosphorylated tau protein, thus inhibition of tau kinases represents a rational approach to treating AD.<sup>3-7</sup> Of particular interest are the KXGS microtubule binding domains in tau as these are thought to control tau/microtubule binding affinity and kinetics.<sup>8</sup> It is speculated that aberrant phosphorylation of the serines in these KXGS motifs acts as a "master switch" leading to high levels of unbound tau and subsequent hyperphosphorylation.<sup>8</sup> Microtubule affinity regulating kinase (MARK) has been demonstrated to be one of the kinases capable of phosphorylation of S262 lying in one of the KXGS binding motifs.<sup>9</sup> It has been speculated elsewhere



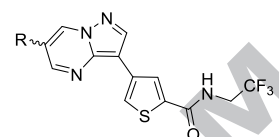
MARK3 IC50 (nM)	1
MARK4 cell IC50 (nM)	50
Kinase selectivity (# < 10-fold vs. MARK)	12 / 101
rat Cl (i.v., mL/min/kg)	32
rat %F	46
rat Vd (L/kg)	14.2

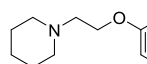
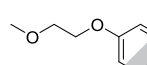
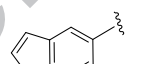
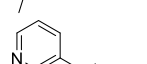
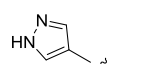
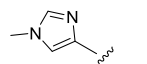
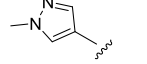
that inhibition of MARK would thus be an attractive therapeutic option for the treatment of Alzheimer's disease.<sup>5</sup> There are four human isoforms of MARK (1-4) and all four are highly enriched in human brain. Additionally, it has been demonstrated that all four isoforms are capable of S262 phosphorylation.<sup>10</sup> Given the high sequence homology, particularly in the ATP binding domain, and the potential of all four isoforms to be pathologically relevant, we sought to identify and optimize pan-MARK inhibitors targeting the ATP binding domain.<sup>10</sup>

Initial efforts in our laboratories led to the identification of compound **1** as a reasonable lead MARK inhibitor for optimization. The compound was potent in both biochemical and cell based assays. Kinase selectivity was less than optimal but pharmacokinetic properties in rats were fair as a starting point. Efforts to measure the susceptibility of **1** to Pgp transport were compromised by the compound's poor physical properties. Of significant concern is the relatively high MW of 529 as CNS penetration tends to be inversely proportional to MW. This manuscript describes our efforts to optimize **1** focusing on improving potency, reducing MW and attaining attributes consistent with CNS penetration.<sup>11</sup>

Modeling of **1** suggests the piperidine group is oriented towards solvent in its bound confirmation. This group likely serves to add solubility to the molecule, but at a significant price to MW and without necessarily improving binding affinity. In an effort to reduce MW, we prepared a series of heterocycle substituted pyrazolopyrimidines (Table 1). Initial truncation of the piperidine to the methoxyethoxy derivative **2** resulted in a slight loss in potency. Bicyclic analogs, **3-5** also resulted in a slight loss in

**Table 1.** Heterocycle substituted pyrazolopyrimidine MARK inhibitors.

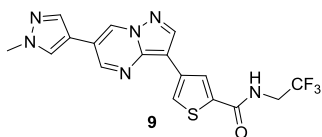


Compound	R	MARK IC <sub>50</sub> (nM)	PSA(A) <sup>2</sup>	MW	LE
1		1	78	529	0.33
2		5	76	476	0.35
3		15	76	444	0.33
4		38	76	442	0.33
5		74	67	455	0.31
6		70	78	403	0.35
7		99	96	392	0.36
8		13	80	406	0.39
9		6	83	406	0.4

potency. Further restriction to the pyridyl or pyrazole substituents again resulted in a loss in potency, but this could be rescued by capping the 5 membered heteroaryl groups **8-9** with a methyl.

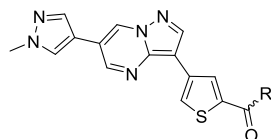
These smaller heterocycles such as methyl imidazole **8** and N-methyl pyrazole **9**, were better tolerated and offered a much better balance of potency to MW as reflected in their increased ligand efficiencies. Given the balance of potency, low MW, and low polar surface area, compound **9** was chosen for further characterization (Figure 2). Despite the inferior biochemical potency of **9** vs. **1**, the cell based activities were quite similar. Selectivity of **9** versus other kinases was still sub-optimal; however the pharmacokinetic parameters in rat were quite good. The compound had modest clearance, good bioavailability and a low volume of distribution. Additionally, **9** was not a Pgp substrate in human or rat and displayed good passive permeability. Upon dose escalation of **9** in rodents, saturation of both C<sub>max</sub> and AUC was observed at relatively low doses, thwarting efforts to look at **9** in a rat hypothermia model of tau S262 phosphorylation. Poor solubility (<3 μM at pH 2 and 7) of this compound was deemed the likely culprit.

**Figure 2.** Properties of MARK inhibitor **9**

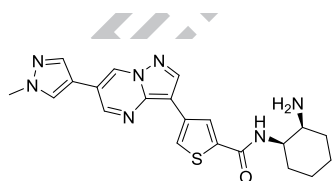


MARK3 IC <sub>50</sub> (nM)	6
MARK4 cell IC <sub>50</sub> (nM)	60
Kinase selectivity (# < 10-fold vs. MARK)	26 / 101
rat Cl (i.v., mL/min/kg)	7.4
rat %F	53
rat Vd (L/kg)	0.77
PGP (B/A:A/B), human/rat	1.4/1.9
Papp (10 <sup>-6</sup> cm/s)	22.6
Solubility μM, pH 7	0

Rather than attempt to address solubility by adding polarity to the solvent exposed region of this class of inhibitors, a strategy that has been demonstrated to be effective but at a cost to molecular weight and ligand efficiency, we decided to focus on the amide portion of **9** (Table 2). The simple ethyl amide **10** had poor activity and highlights the impact of the trifluoromethyl group in compound **9**. Alkyl substituents proximal to the amide bond, such as the cyclopropyl derivative **11**, were able to restore potency to single digit nanomolar range, but also negatively impacted solubility. Cyclic secondary alcohols **12-15** were well tolerated, although these also did little to improve solubility. Cyclic amines **16-21** managed to provide significant improvements in both potency and solubility. The larger, six-membered ring **18-19** was preferred over the smaller cyclopentyl **16-17**, the cis-racemic cyclohexylamine compound **19** demonstrating sub-nanomolar potency. Despite the increase in MW, the potency enhancements observed by the inclusion of this functional group improved the LE to a very respectable 0.43 value. Based on improved potency and solubility, **19** was more fully characterized (Figure 3). We were gratified to see that the improved biochemical potency and physical properties translated into a low single digit nanomolar cellular IC<sub>50</sub>, a first for this program. The kinase selectivity was apparently compromised, but this may also be an artifact of the improved potency



Compound	R	MARK IC <sub>50</sub> (nM)	PSA(A) <sup>2</sup>	MW	LE	Solubility ( $\mu$ M, pH 7)
10		129	81	325	0.38	0
11		9	78	408	0.35	0
12		10	105	408	0.38	0
13		43	104	408	0.35	0
14		24	102	421	0.35	6
15		9	101	421	0.37	0
16		3	108	407	0.43	203
17		2	104	407	0.41	69
18		1	105	421	0.41	193
19		0.5	104	421	0.43	68



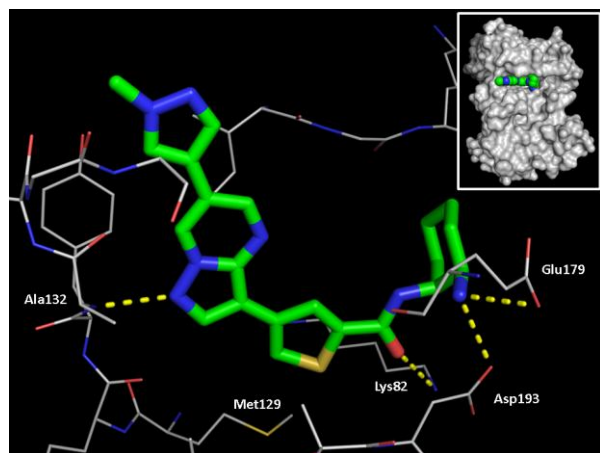
19

MARK3 IC <sub>50</sub> (nM)	<0.5
MARK4 cell IC <sub>50</sub> (nM)	2
Kinase selectivity (# < 10-fold vs. MARK)	24 / 101
rat Cl (i.v., mL/min/kg)	> hepatic
rat Vd (L/kg)	29
PGP (BA:A/B), human/rat	24/54
Papp (10 <sup>-6</sup> cm/s)	13

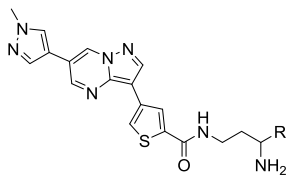
coupled with the screening conditions (biochemical potency is reaching the bottom of assay limits). The rat pharmacokinetic properties were not particularly impressive, with clearance rates greater than hepatic extraction and a high volume of distribution. Not surprising given the increased polarity and basicity, this molecule was also a potent Pgp substrate.

Although **19** was not an ideal candidate for evaluation *in vivo*, we did seek to better understand the source of the potency increase obtained with the novel cyclohexyldiamine amide. Crystallization efforts were commenced with all of the purified MARK isoforms and MARK2 crystals with **19** bound were obtained with good resolution (Figure 4). The overall protein structure is very similar to what has been previously reported,<sup>12</sup> and compound **19** binds in the ATP site extending from the hinge region to the catalytic residues (Figure 4, inset). N1 of the pyrazolopyrimidine core makes a hydrogen bond contact to the hinge backbone NH of Ala132 and the thiophene packs against Met129, the gatekeeper residue. The carbonyl of the amide forms a hydrogen bond to the catalytic Lys82 while the free amine forms a double salt bridge with both Glu179 and Asp193, likely contributing to the high potency. These interactions are accommodated in a manner that enables the cyclohexyl ring to push into the hydrophobic glycine-rich loop. The interactions outlined above are with residues that are highly conserved in the ATP-binding domain of kinases and thus are not likely to offer obvious means of improving selectivity. However, this offers a reasonable means of improving potency and solubility that, at least hypothetically, may be applied to numerous kinase targets. Given the difficulty of attenuating physical properties of ATP-competitive kinase inhibitors, this inhibitor architecture may present a generalizable solution.

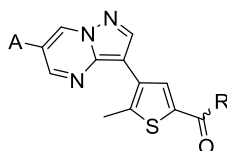
We hypothesized that the poor pharmacokinetics of **19** may, at least in part, be attributable to the relatively high pKa of the free amine.<sup>13-16</sup> To test this hypothesis, a series of 3 amides (**20-22**) with varying calculated amine pKa's were synthesized and evaluated *in vivo* (Figure 5).<sup>17</sup> The amines with lower basicity (**21-22**) led to improved *in vivo* clearance and Pgp ratio. We were now confident that



synthesis of the complex fluorinated cyclohexyldiamine analogs were well worth undertaking. (Table 3). At this point in our program, we had discovered that introduction of a methyl substituent at the 4-position of the thiophene imparted improved kinase selectivity, albeit with decreased overall potency (**23**). Our efforts to address selectivity will be covered in detail in a forthcoming manuscript, but comparative SAR moving forward was conducted with this methyl substituent. Addition of fluoro substituents proximal to the free amine **24**, had a significant negative impact on potency. Surprisingly, addition of the fluorines proximal to the amide NH conferred a significant increase in activity (**25**, R,R-enantiomer was determined to be the most active enantiomer (data not shown). Given this unexpected boost in activity, we reasoned that removal of the N-methylpyrazole, while maintaining good potency, may be possible. Compounds **26** and **27** bear this out as they maintain single digit nanomolar potency

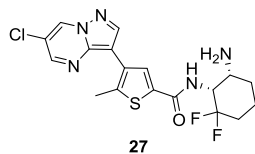


Compound	R	MARK IC <sub>50</sub> (nM)	pKa(Calc)*	rat Cl (i.v., mL/min/kg)	Pgp (hum) BA/AB
20		22	8.4	> hepatic	16.7
21		15	7.4	16.7	11.5
22		10	5.4	14	4.8



Compound	R	A	MARK IC <sub>50</sub> (nM)	PSA(A) <sup>2</sup>	MW	LE	Pgp (hum) BA/AB	Papp	Solubility ( $\mu$ M, pH 7)
23			1.3	102	435	0.39	N/A	N/A	192
	cis, racemic								
24			130.0	101	471	0.29	N/A	N/A	N/A
	S, S								
25			<0.25	102	471	0.40	N/A	N/A	31
	R, R								
26		H	2.4	82	391	0.44	10	26	200
	R, R								
27		Cl	5.0	82	425	0.41	2.9	36	114
	R, R								

with improved ligand binding efficiency. Lower amine pKa along with lower MW and polar surface area are likely contributing factors to achieving Pgp efflux and permeability values that are known to confer CNS penetration, particular in the case of **27**.



MARK3 IC50 (nM)	5
MARK4 cell IC50 (nM)	280
Kinase selectivity (# < 10-fold vs. MARK)	6 / 101
rat Cl (i.v., mL/min/kg)	19
rat Vd (L/kg)	1.3
rat t <sub>1/2</sub> (h)	0.7
dog Cl (i.v., mL/min/kg)	27
dog Vd (L/kg)	2.3
dog t <sub>1/2</sub> (h)	1

Further characterization of the i.v. pharmacokinetic properties of **27** in rat and dog revealed reasonable volumes of distribution but moderate to high clearance and short half-lives (Figure 6). Additionally, the cell-based activity of **27** was less than optimal. While these properties represent an opportunity for further optimization, the solubility of **27** was greatly enhanced by the cumulative modifications starting from lead molecule **1**. At pH 7 **27** attained a concentration of 114  $\mu$ M in our solubility assay and at pH 2 that number increased to 206  $\mu$ M.

We have discussed the identification of an early MARK inhibitor, **1** with high MW and described the optimization of this initial lead through truncation of the polar solvent front substituent. Substitution with small heteroaryls lead to the identification of **9** which maintained potency, but had poor physical properties. In an effort to improve solubility a polar functional cyclohexyldiamine was utilized and shown to have superior potency and physical properties, but suffered from poor PK. By attenuating the basicity of the amine through difluoro-substitution, we were able to improve PK, and serendipitously saw a significant improvement in biochemical and cellular potency. Further discussion on the optimization of compounds similar to **27**, and discussions on the hemodynamic effects associated with the target will be the subject of a future manuscript.<sup>20, 21</sup>

**CORRESPONDING AUTHOR E-MAIL ADDRESS\*:** [david.sloman@merck.com](mailto:david.sloman@merck.com)

## ACKNOWLEDGMENT

We would like to thank Dr. Bruce Adams for NMR support.

## SUPPLEMENTARY DATA

The PDB accession code for the X-ray cocrystal of MARK2 + compound 19 is 5EAK. Supplementary data associated with this article can be found, in the online version, at “ ”<sup>18,19</sup>

## ABBREVIATIONS

AD, Alzheimer's disease; MARK, microtubule affinity regulating kinase; NFT, neurofibrillary tangles; CSF, cerebrospinal fluid; CYP, cytochrome P450; Pgp, P-glycoprotein; LE, ligand efficiency, PSA, polar surface area.

## REFERENCES

- (1) Querfurth, H., W. LaFerla, F. M. *N. Engl. J. Med.* **2010**, 362, 329.
- (2) Citron, M. *Nat. Rev. Drug Discov.* **2010**, 9, 387.
- (3) Gong, C.-X.; Grundke-Iqbal, I.; Iqbal, K. *Drugs Aging* **2010**, 27, 351-365.
- (4) Lee, V. M.-Y.; Brunden, K. R.; Hutton, M.; Trojanowski, J. Q. *Cold Spring Harb. Perspect. Med.* **2011**, 1, a006437

- (5) Martin, L.; Latypova, X.; Wilson, C. M.; Magnaudeix, A.; Perrin, M.L.; Yardin, C.; Terro, F. *Ageing Res. Rev.* **2013**, *12*, 289-309.
- (6) Iqbal, K.; Gong, C.-X.; Liu, F. *Expert Opin. Ther. Tar.* **2014**, *18*, 307-318.
- (7) Drewes, G.; Ebneith, A., Preuss, U., Mandelkow, E.M., and Eckhard Mandelkow b. Lee, V. M.-Y.; Brunden, K. R.; Hutton, M.; Trojanowski, J. Q. *Cell*, **1997**, *89*, 297-308.
- (8) Nishimura, I, Yang, Y., Lu, B., *Cell*, **2004**, *116*, 671-682.
- (9) Matenia, D.; Mandelkow, E.-M. *Trends Biochem. Sci.* **2009**, *34*, 332.
- (10) Timm, T., Marx, A., Panneerselvam, S., Mandelkow, E., Mandelkow, E.M. *BMC Neuroscience*, **2008**, *9*(Suppl 2): S9
- (11) Pajouhesh, H., Lenz, G.R. *NeuroRx*, **2005**, *2*, 541-553.
- (12) Panneerselvam, S., Marx, A., Mandelkow, E. M., Mandelkow E, *Structure*, **2006**, *14*, 173-183.
- (13) Smith, D.; van de Waterbeemd, H.; Walker, D. K. *Pharmacokinetics and Metabolism in Drug Design, 2<sup>nd</sup> Edition*: Mannhold, R.; Kubinyi, H.; Folkers, G. Germany: Wiley-VCH. **2006**.
- (14) Morgenthaler, M.; Schweizer, E.; Hoffmann-Roder, A.; Benini, F.; Martin, R. E.; Jaeschke, G.; Wagner, B.; Fischer, H.; Bendels, S.; Zimmerli, D.; Schneider, J.; Diederich, F.; Kansy, M.; Muller, K. *Chem Med Chem* **2007**, *2*, 1100-1115.
- (15) van Niel, M. B.; Collins, I.; Beer, M. S.; Broughton, H. B.; Cheng, S. K. F.; Goodacre, S. C.; Heald, A.; Locker, K. L.; MacLeod, A. M.; Morrison, D.; Moyes, C. R.; O'Connor, D.; Pike, A.; Rowley, M.; Russel, M. G. N.; Sohal, B.; Stanton, J. A.; Thomas, S.; Verrier, H.; Watt, A. P.; Castro, J. L. *J. Med. Chem.* **1999**, *42*, 2087-2104.
- (16) Hicken E. J.; Marmsater F. P.; Munson M. C.; Schlachter S. T.; Robinson J. E.; Allen S.; Burgess L. E.; DeLisle R. K.; Rizzi J. P.; Topalov G. T.; Zhao, Q.; Hicks J. M.; Kallan, N. C.; Tarlton, E.; Allen, A.; Callejo, M.; Cox, A.; Rana, S.; Klopfenstein, N.; Woessner, R.; Lyssikatos, J.P. *ACS Med. Chem. Lett.* **2014**, *5*, 78-83.
- (17) pKa's calculated using ACD LABS v. 11.0
- (18) \* Some experimentals have been previously reported in; Lim, J.; Taoka, B. M.; Lee, S.; Northrup, A.; Altman, M. D.; Sloman, D. L.; Stanton, M. G.; Noucti, N. Pyrazolo[1,5-a]pyrimidines as mark inhibitors. WO 2011/087999, **2011**.
- (19) \* Some experimentals have been previously reported in; Churcher, I.; Hunt, P.A.; Stanton, M., G. Use of pyrazolo[1,5-a]pyrimidine derivatives for the treatment of Alzheimer's disease and related conditions WO 2007085873 A1 20070802, **2007**.
- (20) Sloman, D. L. Abstracts of Papers, 244th ACS National Meeting & Exposition, Philadelphia, PA, United States, **2012** MEDI-100.
- (21) Lamore, S.D.; Kamendi, H.W.; Scott, C.W.; Dragan, Y.P.; Peters, M.F. *Toxicol. Sci.* **2013**, *135*, 402-413.

## GRAPHICAL ABSTRACT

